BBA - Proteins and Proteomics 1872 (2024) 140969

Contents lists available at ScienceDirect

BBA - Proteins and Proteomics

journal homepage: www.elsevier.com/locate/bbapap

Research Paper

Structure of the *Borrelia burgdorferi* ATP-dependent metalloprotease FtsH in its functionally relevant hexameric form

Kalvis Brangulis [a,b,*], Laura Drunka [a], Inara Akopjana [a], Kaspars Tars [a]

[a] Latvian Biomedical Research and Study Centre, Ratsupites 1 k-1, LV-1067 Riga, Latvia
[b] Department of Human Physiology and Biochemistry, Riga Stradins University, Dzirciema 16, LV-1007 Riga, Latvia

ARTICLE INFO

Keywords:
Lyme borreliosis
Metalloenzyme
AAA+ protease
Spirochetes
X-ray crystallography

ABSTRACT

ATP-dependent proteases FtsH are conserved in bacteria, mitochondria, and chloroplasts, where they play an essential role in degradation of misfolded/unneeded membrane and cytosolic proteins. It has also been demonstrated that the FtsH homologous protein BB0789 is crucial for mouse and tick infectivity and in vitro growth of the Lyme disease-causing agent *Borrelia burgdorferi*. This is not surprising, considering *B. burgdorferi* complex life cycle, residing in both in mammals and ticks, which requires a wide range of membrane proteins and short-lived cytosolic regulatory proteins to invade and persist in the host organism.

In the current study, we have solved the crystal structure of the cytosolic $BB0789_{166–614}$, lacking both N-terminal transmembrane α-helices and the small periplasmic domain. The structure revealed the arrangement of the AAA+ ATPase and the zinc-dependent metalloprotease domains in a hexamer ring, which is essential for ATPase and proteolytic activity. The AAA+ domain was found in an ADP-bound state, while the protease domain showed coordination of a zinc ion by two histidine residues and one aspartic acid residue. The loop region that forms the central pore in the oligomer was poorly defined in the crystal structure and therefore predicted by AlphaFold to complement the missing structural details, providing a complete picture of the functionally relevant hexameric form of BB0789. We confirmed that BB0789 is functionally active, possessing both protease and ATPase activities, thus providing novel structural-functional insights into the protein, which is known to be absolutely necessary for *B. burgdorferi* to survive and cause Lyme disease.

1. Introduction

Borrelia burgdorferi is the causative agent of Lyme disease and can be transferred between infected *Ixodes* ticks and mammalian organisms during the tick's blood meal [31,39]. To function effectively in different host organisms and acquire necessary metabolites, such as amino acids, nucleotides, and lipids, which *B. burgdorferi* cannot synthesize on its own, the pathogen relies on various transmembrane proteins, many of which are transport proteins, including lipoprotein secretion and processing proteins [15]. Lipoproteins, proteins that are covalently attached to fatty acids from the membrane bilayer, are particularly crucial for *B. burgdorferi* to adapt to its environment, as they are involved in tasks such as nutrient binding, attachment to various target receptors, and defence against the immune system. Therefore, the secretion and processing of these proteins must work without interruption [16,24]. To prevent the accumulation of misfolded or unneeded proteins that could disrupt other biological processes, a proteolytic mechanism is essential for removing abnormal membrane proteins and short-lived soluble regulatory proteins. Among several systems capable of regulating protein degradation in bacteria, FtsH stands out because it is a membrane-attached and highly conserved protein degradation system found in bacteria, mitochondria, and chloroplasts of eukaryotes. The absence of this machinery leads to cell death [18,21,22]. Interestingly, FtsH has also been observed to exhibit chaperone activity, which might play an important role in an organism's growth and development, even if the proteolytic activity of FtsH is lost [26,28].

Unlike most other proteases, FtsH consists of two N-terminal transmembrane α-helices that attach the soluble part to the cytosolic side of the cell membrane, which is thought to be important for its ability to interact with membrane proteins [9]. Between the transmembrane helices, there is a small periplasmic α + β domain of about 70 amino acids, which plays a role in the oligomerization of FtsH and its proteolytic activity [1,35]. The soluble cytosolic part of FtsH consists of AAA+ ATPase domain (InterPro entry: IPR003593) from the AAA superfamily

* Corresponding author at: Latvian Biomedical Research and Study Centre, Ratsupites 1 k-1, LV-1067 Riga, Latvia.
E-mail address: kalvis@biomed.lu.lv (K. Brangulis).

https://doi.org/10.1016/j.bbapap.2023.140969
Received 10 August 2023; Received in revised form 13 October 2023; Accepted 13 October 2023
Available online 16 October 2023

(ATPases associated with various cellular activities) and the peptidase M41 domain (InterPro entry: IPR000642) from zinc metalloprotease family. These two domains are linked with a short loop region [40]. The AAA+ domain is found in various proteins across all domains of life, where the energy released from ATP hydrolysis is converted into conformational change that drives diverse processes, including DNA recombination, replication, and repair; protein translocation and unfolding; molecular transport, and cilia/flagella movement [38]. The AAA+ domain contains several characteristic features, including Walker A and B motif that supports ATP binding and hydrolysis, the second region of homology (SRH) involved in oligomerization and ATP hydrolysis, and the FVG motif for target protein recognition and translocation [18,34]. In turn, peptidase M41 domain is characterized by being composed of 8 α-helices (though one of these α-helices is weakly pronounced, and the domain can be considered to be made from 7 α-helices) and a short antiparallel β-ribbon, which together may be regarded as an α-β-α triple sandwich [5]. The first α-helix in the peptidase domain contains the HEXXH motif (where X can be any uncharged residue), and both histidines along with an Asp residue from a different helix (e.g., Asp490 in *E. coli*) coordinate the zinc ion [5]. The zinc ion is essential for the proteolytic activity, and mutations in the histidine residues of the HEXXH motif or the nearby glutamic acid residue, which ensures a proper conformation of the HEXXH motif, disrupt the proteolytic function in FtsH protein [33,43].

In FtsH protein, the AAA+ and zinc protease domains are arranged in a hexameric ring structure. The hexameric state is essential for the proper functioning of the AAA+ and protease domains, as it ensures the formation of a central pore region lined with aromatic residues [5,19]. FtsH recognizes a specific sequence motif in the target protein, known as a degron (which is at least 20 residues long, unstructured, diverse in sequence, and usually located at the N- or C-terminus) to bind to the pore region [10]. As a result of conformational caused by ATP hydrolysis, the target protein is translocated in an unfolded state to the active site of the zinc-dependent protease [4]. The hydrolysis of the target protein leads to peptide fragments with an average size of 10 residues, which then escape from the hexameric complex through openings in the side [34]. The unfoldase activity, generated by the pulling forces during ATP hydrolysis, is particularly effective against membrane proteins due to geometric constraints resulting from the close proximity of the cytosolic FtsH hexamer to the membrane [17,20]. Recently, it has been revealed that four FtsH hexamers are assembled together with the help of the scaffolding proteins HflK/C, as the transmembrane helices of HflK/C surround and seal the FtsH complex. However, in the case of *B. burgdorferi*, the loss of HflK/C did not affect the physiology of the bacterium [11,27].

To gain both structural and functional insights into the protein that is known to play an essential role in the ability of *B. burgdorferi* to survive and cause Lyme disease, we determined the crystal structure of the soluble FtsH homologous protein BB0789. One of our aims was to assess its similarity to other FtsH proteins and to identify the presence of the key residues necessary for translocation and proteolytic activity. As mentioned earlier, FtsH in some organisms has lost its proteolytic activity while still retaining an essential role [28]. Therefore, we conducted experiments to confirm that *Borrelia* FtsH homologous protein BB0789 indeed functions as an ATP-driven protease.

2. Materials and methods

2.1. Cloning, expression and purification of BB0789

To produce recombinant $BB0789_{146–639}$ (UniProtKB: O51729), corresponding to the protein region containing the putative AAA+ ATPase and peptidase M41 domain, a gene from genomic *B. burgdorferi* B31 DNA was amplified by PCR using the following primers: 5′CAT GCC ATG GGC GGC GGT GGG AAG GTT TTT -3′ and 5′-GCT TGC GGC CGC TTA ACC TTT TAC ATC CTC CCC -3′ (*NcoI* and *NotI* recognition sites in the primers are underlined). The product was ligated into the pETm-11 expression vector, resulting in a construct encoding an N-terminal 6xHis tag followed by a tobacco etch virus (TEV) protease cleavage site. The protein was expressed in *Escherichia coli* BL21(DE3) using the same approach as previously described for *B. burgdorferi* protein BBE31 [7]. For Se-Met protein expression, a similar method was employed as previously described for *B. burgdorferi* BB0689 [8]. After expression, the protein was purified using affinity chromatography, and the 6xHis tag was removed by proteolytic cleavage, following a procedure similar to that described previously for BBA65 and BSA64 [6]. To prepare the protein for subsequent crystallization, it was concentrated to 10 mg/ml by using an Amicon centrifugal filter unit (Millipore, Burlington, MA, USA).

2.2. Crystallization of BB0789

BB0789 was crystallized in 96-well sitting drop plates (SWISSCI AG, Neuheim, Switzerland) by using the 96-reagent sparse-matrix screens JCSG+ and Structure Screen 1&2 (Molecular Dimensions, Newmarket, UK). A total of 0.4 μl of protein at a concentration of 10 mg/ml was mixed with 0.4 μl of precipitant using a Tecan Freedom EVO100 workstation (Tecan Group, Männedorf, Switzerland). After extensive manual optimization of the crystallization conditions, cubic-shaped crystals were obtained. These crystals appeared after 2–3 days in a precipitant solution containing 0.2 M sodium citrate tribasic dehydrate, 0.1 M Tris (pH 8.5), and 28% PEG 400. The crystals selected for data collection were subjected to cryoprotection by increasing the concentration of PEG 400 in the mother liquor to 35% and then frozen in liquid nitrogen.

2.3. Data collection and structure determination

Diffraction data for Se-Met *B. burgdorferi* BB0789 were collected at *the MX beamline instrument BL 14.1 at Helmholtz-Zentrum, Berlin* [29]. Reflections were indexed by MOSFLM and scaled by AIMLESS from the CCP4 suite [3,14,44]. The initial phases were obtained by SHELX C/D/E [36]. The initial protein model was built automatically in BUCCANEER and improved by manual rebuilding in COOT [12,13]. Crystallographic refinement was performed using REFMAC5 [30]. A summary of the data collection, refinement and validation statistics for BB0789 is given in Table 1. AlphaFold v2.0 [23] was used to predict the 3D structure for *B. burgdorferi* BB0789 and FtsH proteins from *Leptospira santarosai* and *Treponema pallidum* using our local processing hardware as described previously [2].

2.4. ATPase and protease activity assays

The measurement of ATPase activity was conducted using the colorimetric ATPase Assay Kit from Abcam (Cambridge, UK), following the manufacturer's instructions. In a 96-well plate, 4 μl of protein solution (4.3 mg/ml) was combined with 96 μL of ATPase assay buffer and 100 μL of a reaction mix containing the ATPase substrate. The reaction mixture was then incubated at 25 °C for a duration of 30 min. Following this, 30 μl of ATPase assay developer (containing malachite green) was added and allowed to incubate for an additional 30 min at 25 °C. The formation of a dark green-colored complex, resulting from the interaction between malachite green and the inorganic phosphate released during ATP hydrolysis was assessed by measuring the absorbance at 650 nm using a microplate reader.

For the measurement of protease activity, the Protease Activity Assay Kit (Abcam, Cambridge, UK) was used, which employs fluorescein isothiocyanate (FITC)-labeled casein as a substrate. The assay was carried out in accordance with the manufacturer's instructions. Briefly, protein solutions at concentrations of 0.5, 1.0 and 2 μM (final concentration) were mixed with 10 mM ATP, 20 mM $MgCl_2$, assay buffer, and the reaction mix. The fluorescence intensity was measured at Ex/Em = 485/530 nm initially and then re-measured after the reaction mixture was

Table 1
Statistics for Data and Structure Quality.

Dataset	BB0789
X-ray diffraction data	
PDB entry	7ZBH
Beamline	14.1 BESSY II, Helmholtz-Zentrum, Berlin
Space group	C 2_1
a, *b*, *c* (Å)	153.8, 192.8, 114.1
α, *β*, *γ* (°)	90.0, 124.3, 90.0
Wavelength (Å)	0.91840
Resolution (Å)	96.56–3.30
Highest resolution bin (Å)	3.43–3.00
No. of reflections	155,533
No. of unique reflections	40,345
Completeness (%)	97.9 (99.0)
R_{merge}	0.03 (0.29)
$CC_{1/2}$	0.99 (0.89)
I/σ (*I*)	16.3 (2.9)
Multiplicity	3.9 (3.9)
Refinement	
R_{work}	0.278 (0.359)
R_{free}	0.331 (0.405)
Average B-factor (Å^2)	
Overall	118.1
From Wilson plot	106.1
No. of atoms	
Protein	16,396
Water	0
RMS deviations from ideal	
Bond lengths (Å)	0.006
Bond angles (°)	1.432
Ramachandran outliers (%)	
Residues in most favored regions (%)	90.26
Residues in allowed regions (%)	7.47
Outliers (%)	2.27

Values in parentheses are for the highest resolution bin.

incubated in the dark at 25 °C for 30 min.

3. Results and discussion

3.1. Overall structure of BB0789

The crystal structure of recombinant *B. burgdorferi* $BB0789_{146–639}$, lacking both N-terminal transmembrane helices and the periplasmic domain, was successfully solved. The resolved region covers residues 169–603, as the electron density for the first 23 residues and the last 36 residues in $BB0789_{146–639}$ was not observed (Fig. 1). The probable reason for this observation is that residues 146 to 168 form a loop region following the second transmembrane α-helix, which connects the α-helix within the membrane to the cytosolic structural domain. Consequently, these loop residues are not well-defined in the crystal structure. At the C-terminal end, residues 604–639 correspond to an unstructured region as predicted by AlphaFold structure of the full-length BB0789 (Fig. 2A). This unstructured region lacks a well-defined secondary structure and remains flexible in the crystal structure.

Additionally, the electron density was poorly defined for several loop regions. As a result, the backbone for the following residues was not built: Glu243, Gly277-Gly287, Gly306-Asn310, Asn396-Asp404, Met414-Ile423, Arg461-Leu475 and Asp538-Lys553 (Fig. 1). The crystals of $BB0789_{146–639}$ belonged to the space group C2, with six monomers per asymmetric unit. Notably, all six monomers were organized in a biologically relevant hexameric ring-like structure. The hexameric assembly had a diameter of approximately 110 Å and height of 60 Å (Fig. 3A). This hexameric arrangement is significant as it is crucial for the proper function of the protein, given its role as an ATP-driven protease.

In the hexameric structure of recombinant *B. burgdorferi* FtsH homologous protein BB0789, each monomer is composed of an AAA+ domain and a protease domain. These domains give rise to two distinct rings within the hexamer. The AAA+ domain is located towards the N-terminus and the substrate enters FtsH through the AAA+ domain, therefore it can be considered as the upper layer, whereas the protease forms the bottom layer. In the crystal structure, certain loop regions, including the loop region that forms the central core region of the hexameric structure, were not well-defined due to weak electron density. To complement the experimental data, the AlphaFold predicted model of BB0789 was used. However, the mutual positions of the AAA+ and protease domains in the AlphaFold predicted structure did not match what was observed in the crystal structure (Fig. 2B). This discrepancy can be attributed to the flexibility of the loop region between both domains, which was reflected by a low AlphaFold per-residue confidence score or pLDDT [41] for that specific region (pLDDT <80). To address this, the crystal structure of BB0789 was superimposed with the separated AAA+ and protease domains of the predicted BB0789 (Fig. 3B). The predicted structures of the individually

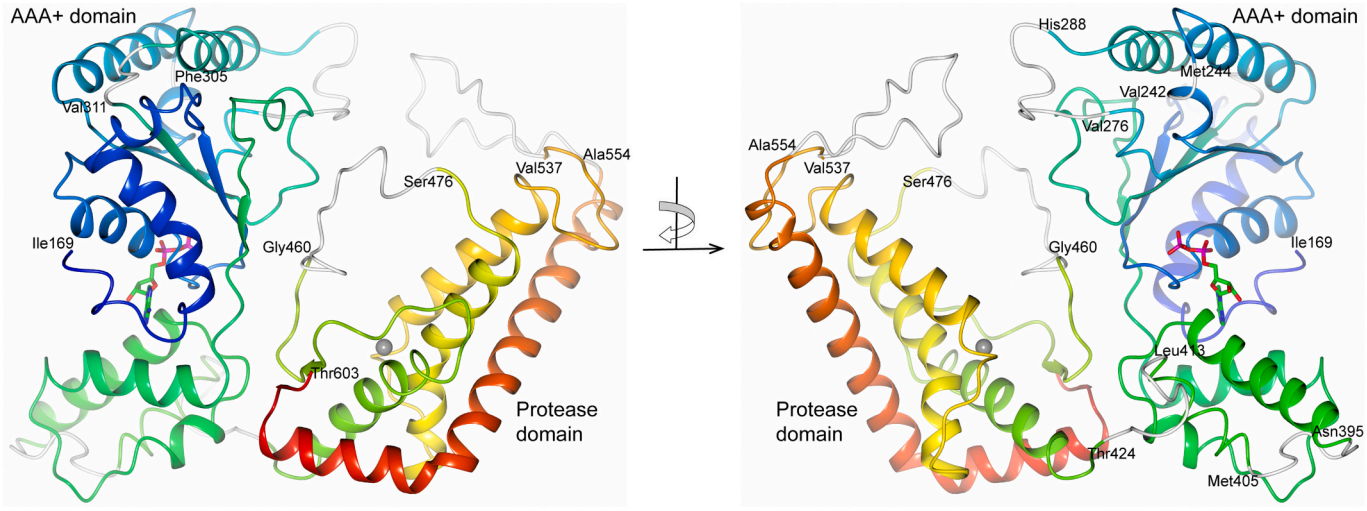

Fig. 1. The crystal structure of *B. burgdorferi* BB0789 (PDB ID 7ZBH). The structure is displayed in two different angles, rotated by 180 degrees. The coloring scheme goes from blue at the N-terminus to red at the C-terminus, representing the sequence direction. In the structure, a zinc ion is illustrated as a grey sphere, while ADP is represented as a ball-and-stick model, with carbon atoms in green, oxygen atoms in red, and nitrogen atoms in blue. The loop regions that showed poor electron density, and therefore, the backbone was not built are illustrated in white colour. The residues corresponding to the terminal parts of the missing fragments are indicated in the structure. (For interpretation of the references to colour in this figure legend, the reader is referred to the web version of this article.)

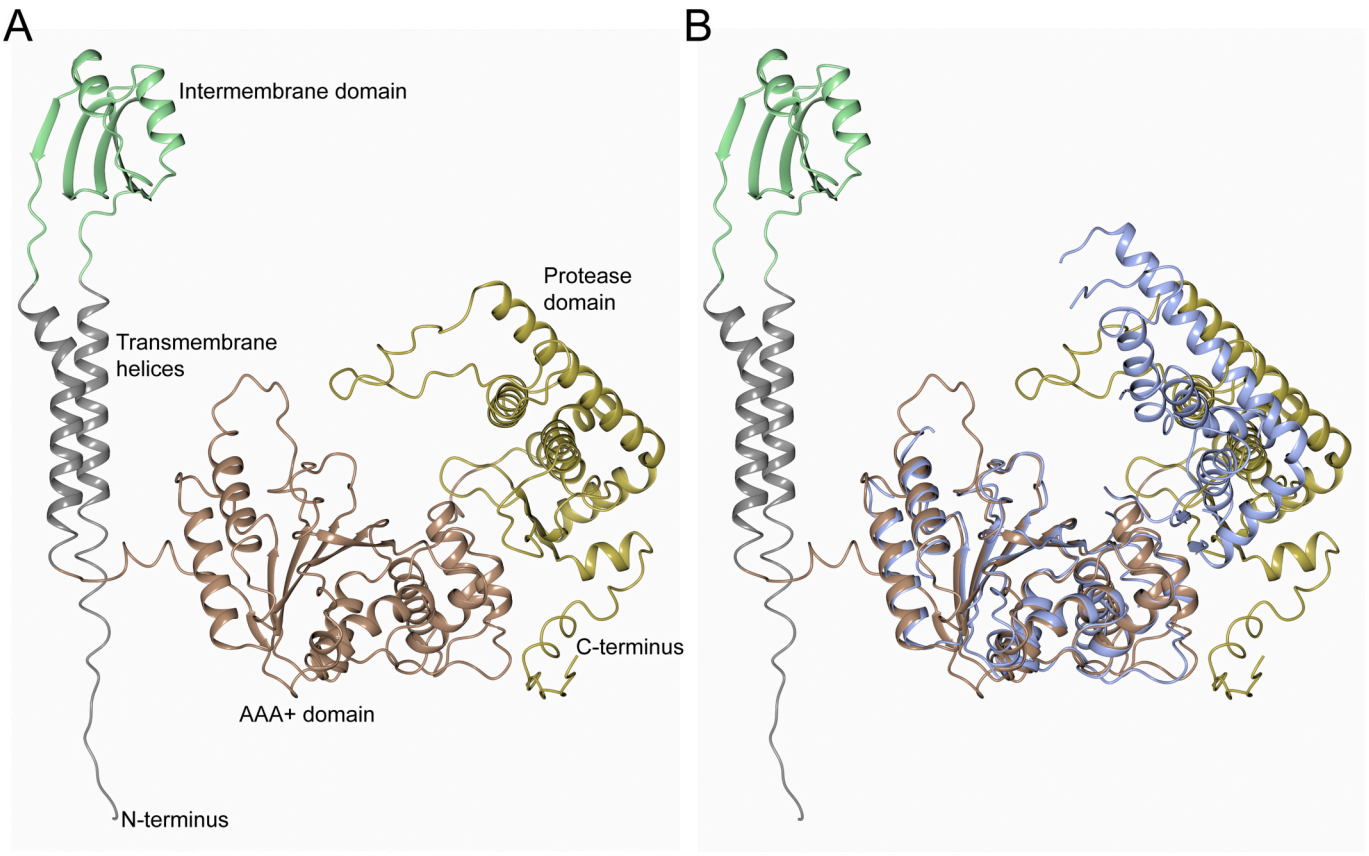

Fig. 2. The predicted structure of full-length *B. burgdorferi* BB0789 and comparison to the crystal structure of $BB0789_{146–639}$. (A) The predicted structure of full-length *B. burgdorferi* BB0789. BB0789 is colored according to protein domains/segments as named in the fig. (B) Superimposed full-length structure of BB0789 with the crystal structure of $BB0789_{146–639}$ (C^{α} root-mean-square deviation of 1.90 Å over 232 residues). $BB0789_{146–639}$ is colored in blue. (For interpretation of the references to colour in this figure legend, the reader is referred to the web version of this article.)

superimposed AAA+ and protease domains exhibited very high similarity to the crystal structure (RMSD 0.92 Å). Additionally, the predicted structure provided valuable insight into the loop regions in the central part of the hexamer that were not visible in the crystal structure (Fig. 3C). This complemented the experimental data and offered a more comprehensive understanding of the protein's structure.

The interactions between the monomers in the hexameric complex of BB0789 are primarily polar, with a few additional hydrophobic interactions. Due to the flexibility of the AAA+ domain in FtsH proteins, the binding between the protease domains is more dominant. This binding involves specific residues, such as Tyr490, Tyr493, Gln508, Asp561 and Lys568 (Fig. 3D).

In the crystal structure of BB0789, each AAA+ domain is found in an ADP-bound state. The interaction between ADP and the AAA+ domain is mainly mediated by backbone NH groups from residues Gly215, Thr216, Lys218, Thr219, Leu220, and Ala379 (Fig. 4). In addition to the ADP-binding site, the crystal structure reveals the coordination of a zinc ion within the protease domain. The zinc ion is coordinated by specific residues, namely His434, His438, and Asp510 (Fig. 4).

3.2. *B. burgdorferi BB0789 as an FtsH*

In *B. burgdorferi*, the FtsH homologous protein BB0789 is encoded by a single gene located on a chromosome, similar to the gene organization in most other bacteria. For instance, orthologs of BB0789 can be identified in other spirochetes, where a single gene is also responsible for encoding this protein, and the overall structure remains highly conserved (Supplementary Fig. S1). When comparing the crystal structure of BB0789 with other structures deposited in the Protein Data Bank (PDB) using the PDBeFold tool [25], it revealed structural matches with ATP-dependent zinc metalloprotease FtsH from three different organisms (Table 2).

The three FtsH proteins from different organisms, including *A. aeolucis*, *T. maritima*, and *T. thermophilus*, have been experimentally confirmed to be active proteases based on ATPase and protease activity assays [5,40,42]. When the crystal structures of these FtsH proteins were superimposed with the crystal structure of BB0789, it revealed that the overall architecture is highly similar, including the positions of ADP and the zinc ion (Fig. 5B and Table 2).

As mentioned previously, both the AAA+ domain and the protease domain in FtsH proteins are known to contain several characteristic motifs that are essential for their structural and functional integrity [18]. The AAA+ domain possesses essential motifs such as the Walker A and B motif, the SRH motif and the FVG motif. Similarly, the protease domain contains the HEXXH motif, which is important for coordinating the zinc ion and thereby facilitating the proteolytic activity. By performing a multiple sequence alignment of BB0789 with FtsH proteins from *A. aeolucis*, *T. maritima* and *T. thermophilus* and conducting structural analysis, it was confirmed that *B. burgdorferi* BB0789 possesses all of these characteristic motifs. Furthermore, these regions in BB0789 contain all of the functionally important residues (Fig. 5A and C).

The observation that the residues in BB0789 found at the interface between the monomers in the hexameric structure are not conserved with the other FtsH proteins (as indicated in Figs. 3D and 5A) is noteworthy.

While BB0789 has been shown to be essential for *B. burgdorferi* viability [11], it is important to recognize that in some organisms, FtsH proteins have lost their proteolytic activity but still retain novel and

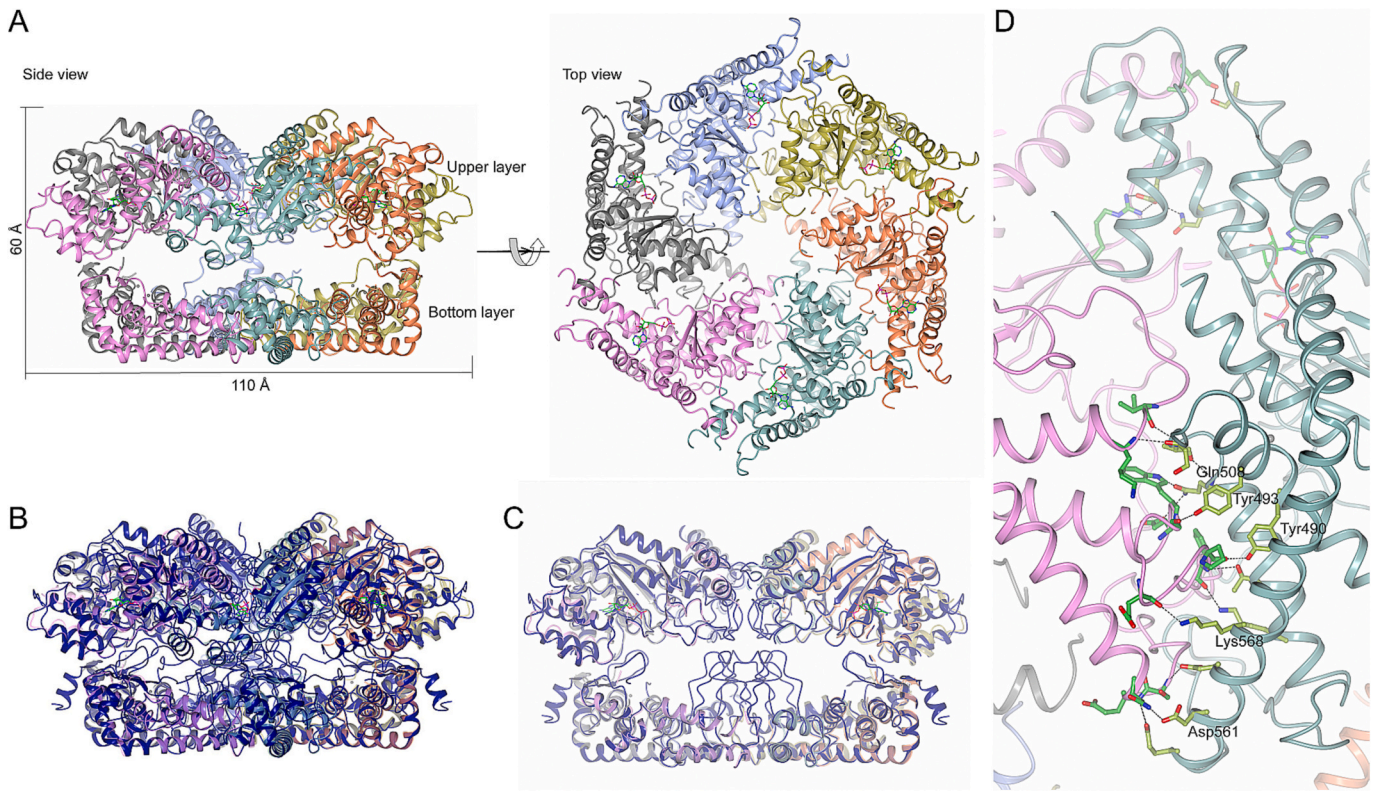

Fig. 3. (A) The hexameric ring-like structure of *B. burgdorferi* BB0789 is illustrated in both side and top views. Each monomer is presented in different colour, allowing for clear visualization of the individual subunits. (B) The crystal structure of BB0789 is superimposed with the predicted structure of BB0789. The predicted structure is shown in blue, while each monomer in the crystal structure is in a different colour. (C) The central part of the superimposed crystal structure and predicted structure hexamer is displayed, highlighting the core-forming loop region. (D) An interface between two monomers from the hexameric structure is illustrated, showing the residues involved in the interaction. One of the monomers is colored pink, while the other is green. The carbon atoms in the residues are colored accordingly to facilitate visualization. (For interpretation of the references to colour in this figure legend, the reader is referred to the web version of this article.)

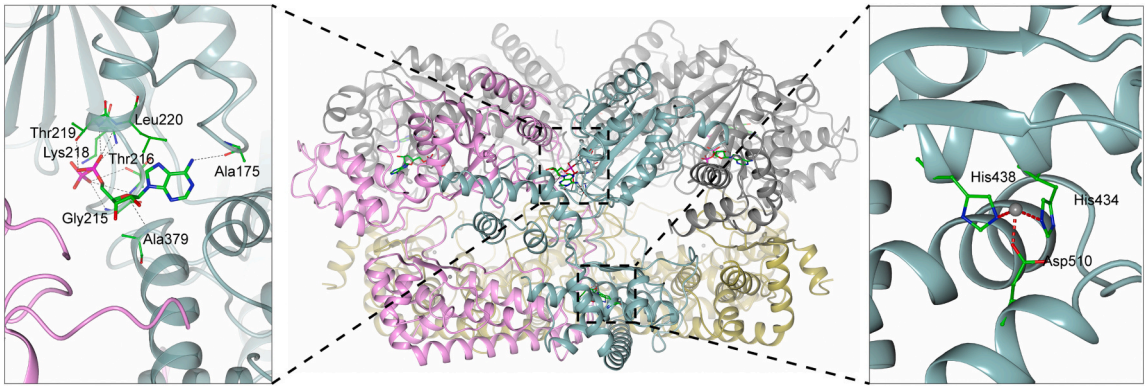

Fig. 4. The crystal structure of BB0789 hexamer with ADP binding site illustrated on the left and zinc binding site on the right. The residues involved in the interaction with ADP and zinc are illustrated.

Table 2
PDBeFold search results against BB0789.

No.	Protein	Organism	PDB ID	*Z*-score	RMSD (Å)	Identity (%)	N residues
1.	ATP-dependent zinc metalloprotease FtsH (Uniprot: O67077)	*Aquifex aeolicus*	6gco	15.4	1.75	47.3	339
2.	ATP-dependent zinc metalloprotease FtsH (Uniprot: Q9WZ49)	*Thermotoga maritima*	2cea	15.3	3.03	47.5	292
3.	ATP-dependent zinc metalloprotease FtsH (Uniprot: Q5SI82)	*Thermus thermophilus*	2dhr	10.6	2.80	46.1	319

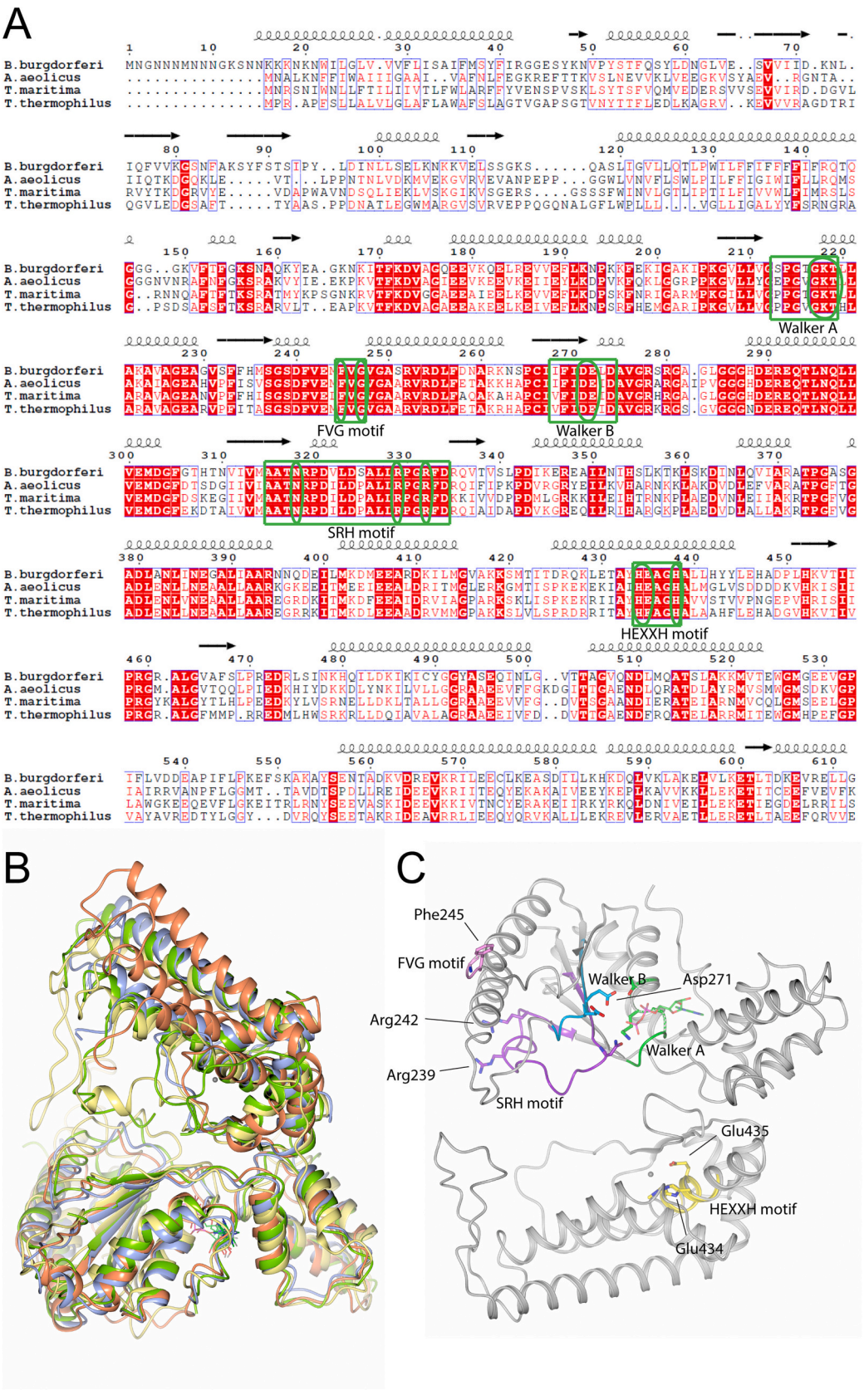

(caption on next page)

Fig. 5. Evaluation of BB0789 as an FtsH protease. (A) The sequence alignment of *B. burgdorferi* BB0789 (UniProt O51729) with FtsH proteins from *A. aeolicus* (UniProt O67077), *T. maritima* (UniProt Q9WZ49), and *T. thermophilus* (UniProt Q5SI82). The alignment was generated using *Clustal Omega*, and the processed sequence data was visualized using ESPript 3 [32,37]. Highly conserved residues between these paralogous proteins are highlighted with a red background, while residues conserved only among separate members are shown in red and framed in blue. The motifs in the alignment are indicated with a green square, and residues within the motifs that are known to be functionally important are circled. The locations of secondary structure elements and the residue numbers for BB0789 are provided above the alignment. (B) The crystal structure of *B. burgdorferi* BB0789 (blue) is superimposed with the crystal structures of FtsH from *A. aeolucis* (PDB ID 6gco, green), *T. maritima* (PDB ID 2cea, orange), and *T. thermophilus* (PDB ID 2dhr, yellow). (C) The Walker A and B motif, the SRH motif, the FVG motif, and the HEXXH motif in BB0789 are indicated. (For interpretation of the references to colour in this figure legend, the reader is referred to the web version of this article.)

critical functions [28]. The multifunctionality of FtsH proteins in different organisms highlights their versatility in biological processes and underscores the complexity of their roles within cellular pathways. To confirm that BB0789 is indeed an ATP-dependent protease, enzymatic activity assay was conducted using fluorescein isothiocyanate-labeled casein as a substrate. According to the fluorescence assay conducted using concentrations of 0.5 μM, 1.0 μM, and 2 μM of BB0789, the enzyme activity of 0.022 mU/ml was detected. This assay is a standard method to assess protease activity, and its successful demonstration with BB0789 further supports its classification as an ATP-dependent protease. Additionally, colorimetric ATPase activity test indicated that BB0789 is able to hydrolyze ATP releasing ADP and a free phosphate ion. Together, the combination of structural, sequence, and enzymatic activity data provides a comprehensive understanding of BB0789 as an FtsH protease and sheds light on its significance in *B. burgdorferi's* survival and pathogenicity.

4. Conclusions

Our study provides further insights into the ATP-dependent protease FtsH homologous protein BB0789 from *B. burgdorferi*, which plays a crucial role in the survival and pathogenicity of Lyme disease causing agent. By solving the crystal structure of the cytosolic region of BB0789 we revealed the essential hexameric ring arrangement of the AAA+ ATPase and the zinc-dependent metalloprotease domains, which is critical for its ATPase and proteolytic activities. We showed that BB0789 contains all the structural motifs found in functional ATP-dependent proteases and we confirmed that BB0789 is functionally active, possessing both protease and ATPase activities further emphasizing its significance in the degradation of misfolded/unneeded membrane and cytosolic proteins in *B. burgdorferi*. Overall, the elucidation of the crystal structure and functional characterization of BB0789 enhances our understanding of the molecular mechanisms underlying the infectivity and survival of the pathogen in both mammalian hosts and ticks. This knowledge may have significant implications for the development of novel therapeutic strategies against Lyme disease, targeting BB0789 as a potential key component of the pathogen's survival machinery.

Supplementary data to this article can be found online at https://doi.org/10.1016/j.bbapap.2023.140969.

Accession numbers

The coordinates and the structure factors for *B. burgdorferi* BB0789 have been deposited in the Protein Data Bank with the accession number 7ZBH.

CRediT authorship contribution statement

Kalvis Brangulis: Conceptualization, Funding acquisition, Investigation, Methodology, Project administration, Resources, Supervision, Validation, Writing – original draft, Writing – review & editing. **Laura Drunka:** Investigation. **Inara Akopjana:** Investigation. **Kaspars Tars:** Writing – review & editing.

Declaration of Competing Interest

The authors declare no conflicts of interest.

Data availability

Data will be made available on request.

Acknowledgments

This work was supported by the European Regional Development Fund grant 1.1.1.1/20/A/048. Diffraction data for *B. burgdorferi* BB0789 were collected on BL14.1 at the BESSY II electron storage ring operated by the Helmholtz-Zentrum, Berlin. We would particularly like to acknowledge the help and support of Manfred S. Weiss and Jan Wollenhaupt during the experiment.

References

[1] Y. Akiyama, A. Kihara, H. Mori, T. Ogura, K. Ito, Roles of the periplasmic domain of Escherichia coli FtsH (HflB) in protein interactions and activity modulation, J. Biol. Chem. 273 (1998) 22326–22333.
[2] I. Akopjana, K. Brangulis, Structural analysis of the outer membrane lipoprotein BBA14 (OrfD) and the corresponding paralogous gene family 143 (PFam143) from Borrelia burgdorferi, Pathogens 11 (2022).
[3] T.G. Battye, L. Kontogiannis, O. Johnson, H.R. Powell, A.G. Leslie, iMOSFLM: a new graphical interface for diffraction-image processing with MOSFLM, Acta Crystallogr. D Biol. Crystallogr. 67 (2011) 271–281.
[4] C. Bieniossek, B. Niederhauser, U.M. Baumann, The crystal structure of apo-FtsH reveals domain movements necessary for substrate unfolding and translocation, Proc. Natl. Acad. Sci. U. S. A. 106 (2009) 21579–21584.
[5] C. Bieniossek, T. Schalch, M. Bumann, M. Meister, R. Meier, U. Baumann, The molecular architecture of the metalloprotease FtsH, Proc. Natl. Acad. Sci. U. S. A. 103 (2006) 3066–3071.
[6] K. Brangulis, I. Akopjana, I. Petrovskis, A. Kazaks, K. Tars, Structural analysis of the outer surface proteins from Borrelia burgdorferi paralogous gene family 54 that are thought to be the key players in the pathogenesis of Lyme disease, J. Struct. Biol. 210 (2020), 107490.
[7] K. Brangulis, I. Akopjana, I. Petrovskis, A. Kazaks, D. Zelencova, A. Jekabsons, K. Jaudzems, K. Tars, BBE31 from the Lyme disease agent Borrelia burgdorferi, known to play an important role in successful colonization of the mammalian host, shows the ability to bind glutathione, Biochim. Biophys. Acta Gen. Subj. 129499 (2019).
[8] K. Brangulis, K. Jaudzems, I. Petrovskis, I. Akopjana, A. Kazaks, K. Tars, Structural and functional analysis of BB0689 from Borrelia burgdorferi, a member of the bacterial CAP superfamily, J. Struct. Biol. 192 (2015) 320–330.
[9] V. Carvalho, I. Prabudiansyah, L. Kovacik, M. Chami, R. Kieffer, R. van der Valk, N. de Lange, A. Engel, M.E. Aubin-Tam, The cytoplasmic domain of the AAA+ protease FtsH is tilted with respect to the membrane to facilitate substrate entry, J. Biol. Chem. 296 (2021), 100029.
[10] S. Chiba, Y. Akiyama, K. Ito, Membrane protein degradation by FtsH can be initiated from either end, J. Bacteriol. 184 (2002) 4775–4782.
[11] C.Y. Chu, P.E. Stewart, A. Bestor, B. Hansen, T. Lin, L. Gao, S.J. Norris, P.A. Rosa, Function of the *Borrelia burgdorferi* FtsH homolog is essential for viability both in vitro and in vivo and independent of HflK/C, mBio 7 (2016) e00404–e00416.
[12] K. Cowtan, The Buccaneer software for automated model building. 1. Tracing protein chains, Acta Crystallogr. D Biol. Crystallogr. 62 (2006) 1002–1011.
[13] P. Emsley, K. Cowtan, Coot: model-building tools for molecular graphics, Acta Crystallogr. D Biol. Crystallogr. 60 (2004) 2126–2132.
[14] P.R. Evans, An introduction to data reduction: space-group determination, scaling and intensity statistics, Acta Crystallogr. D Biol. Crystallogr. 67 (2011) 282–292.
[15] C.M. Fraser, S. Casjens, W.M. Huang, G.G. Sutton, R. Clayton, R. Lathigra, O. White, K.A. Ketchum, R. Dodson, E.K. Hickey, M. Gwinn, B. Dougherty, J. F. Tomb, R.D. Fleischmann, D. Richardson, J. Peterson, A.R. Kerlavage, J. Quackenbush, S. Salzberg, M. Hanson, R. van Vugt, N. Palmer, M.D. Adams, J. Gocayne, J. Weidman, T. Utterback, L. Watthey, L. McDonald, P. Artiach, C. Bowman, S. Garland, C. Fuji, M.D. Cotton, K. Horst, K. Roberts, B. Hatch, H. O. Smith, J.C. Venter, Genomic sequence of a Lyme disease spirochaete, Borrelia burgdorferi, Nature 390 (1997) 580–586.
[16] D.A. Haake, Spirochaetal lipoproteins and pathogenesis, Microbiology (Reading) 146 (Pt 7) (2000) 1491–1504.
[17] C. Herman, S. Prakash, C.Z. Lu, A. Matouschek, C.A. Gross, Lack of a robust unfoldase activity confers a unique level of substrate specificity to the universal AAA protease FtsH, Mol. Cell 11 (2003) 659–669.

[18] K. Ito, Y. Akiyama, Cellular functions, mechanism of action, and regulation of FtsH protease, Annu. Rev. Microbiol. 59 (2005) 211–231.
[19] T. Yamada-Inagawa, T. Okuno, K. Karata, K. Yamanaka, T. Ogura, Conserved pore residues in the AAA protease FtsH are important for proteolysis and its coupling to ATP hydrolysis, J. Biol. Chem. 278 (2003) 50182–50187.
[20] Y. Yang, R. Guo, K. Gaffney, M. Kim, S. Muhammednazaar, W. Tian, B. Wang, J. Liang, H. Hong, Folding-degradation relationship of a membrane protein mediated by the universally conserved ATP-dependent protease FtsH, J. Am. Chem. Soc. 140 (2018) 4656–4665.
[21] L. Yi, B. Liu, P.J. Nixon, J. Yu, F. Chen, Recent advances in understanding the structural and functional evolution of FtsH proteases, Front. Plant Sci. 13 (2022), 837528.
[22] H. Janska, M. Kwasniak, J. Szczepanowska, Protein quality control in organelles - AAA/FtsH story, Biochim. Biophys. Acta 1833 (2013) 381–387.
[23] J. Jumper, R. Evans, A. Pritzel, T. Green, M. Figurnov, O. Ronneberger, K. Tunyasuvunakool, R. Bates, A. Zidek, A. Potapenko, A. Bridgland, C. Meyer, S.A. A. Kohl, A.J. Ballard, A. Cowie, B. Romera-Paredes, S. Nikolov, R. Jain, J. Adler, T. Back, S. Petersen, D. Reiman, E. Clancy, M. Zielinski, M. Steinegger, M. Pacholska, T. Berghammer, S. Bodenstein, D. Silver, O. Vinyals, A.W. Senior, K. Kavukcuoglu, P. Kohli, D. Hassabis, Highly accurate protein structure prediction with AlphaFold, Nature 596 (2021) 583–589.
[24] M.R. Kenedy, T.R. Lenhart, D.R. Akins, The role of Borrelia burgdorferi outer surface proteins, FEMS Immunol. Med. Microbiol. 66 (2012) 1–19.
[25] E. Krissinel, K. Henrick, Secondary-structure matching (SSM), a new tool for fast protein structure alignment in three dimensions, Acta Crystallogr. D Biol. Crystallogr. 60 (2004) 2256–2268.
[26] W. Li, D.K. Rao, P. Kaur, Dual role of the metalloprotease FtsH in biogenesis of the DrrAB drug transporter, J. Biol. Chem. 288 (2013) 11854–11864.
[27] C. Ma, C. Wang, D. Luo, L. Yan, W. Yang, N. Li, N. Gao, Structural insights into the membrane microdomain organization by SPFH family proteins, Cell Res. 32 (2022) 176–189.
[28] L.S. Mishra, C. Funk, The FtsHi enzymes of Arabidopsis thaliana: pseudo-proteases with an important function, Int. J. Mol. Sci. 22 (2021).
[29] U. Mueller, N. Darowski, M.R. Fuchs, R. Forster, M. Hellmig, K.S. Paithankar, S. Puhringer, M. Steffien, G. Zocher, M.S. Weiss, Facilities for macromolecular crystallography at the Helmholtz-Zentrum Berlin, J. Synchrotron Radiat. 19 (2012) 442–449.
[30] G.N. Murshudov, A.A. Vagin, E.J. Dodson, Refinement of macromolecular structures by the maximum-likelihood method, Acta Crystallogr. D Biol. Crystallogr. 53 (1997) 240–255.
[31] J.D. Radolf, M.J. Caimano, B. Stevenson, L.T. Hu, Of ticks, mice and men: understanding the dual-host lifestyle of Lyme disease spirochaetes, Nat. Rev. Microbiol. 10 (2012) 87–99.
[32] X. Robert, P. Gouet, Deciphering key features in protein structures with the new ENDscript server, Nucleic Acids Res. 42 (2014) W320–W324.
[33] N. Saikawa, K. Ito, Y. Akiyama, Identification of glutamic acid 479 as the gluzincin coordinator of zinc in FtsH (HflB), Biochemistry 41 (2002) 1861–1868.
[34] R.T. Sauer, T.A. Baker, AAA+ proteases: ATP-fueled machines of protein destruction, Annu. Rev. Biochem. 80 (2011) 587–612.
[35] F. Scharfenberg, J. Serek-Heuberger, M. Coles, M.D. Hartmann, M. Habeck, J. Martin, A.N. Lupas, V. Alva, Structure and evolution of N-domains in AAA metalloproteases, J. Mol. Biol. 427 (2015) 910–923.
[36] G.M. Sheldrick, A short history of SHELX, Acta Crystallogr. A 64 (2008) 112–122.
[37] F. Sievers, A. Wilm, D. Dineen, T.J. Gibson, K. Karplus, W. Li, R. Lopez, H. McWilliam, M. Remmert, J. Soding, J.D. Thompson, D.G. Higgins, Fast, scalable generation of high-quality protein multiple sequence alignments using clustal omega, Mol. Syst. Biol. 7 (2011) 539.
[38] J. Snider, G. Thibault, W.A. Houry, The AAA+ superfamily of functionally diverse proteins, Genome Biol. 9 (2008) 216.
[39] A.C. Steere, J. Coburn, L. Glickstein, The emergence of Lyme disease, J. Clin. Invest. 113 (2004) 1093–1101.
[40] R. Suno, H. Niwa, D. Tsuchiya, X. Zhang, M. Yoshida, K. Morikawa, Structure of the whole cytosolic region of ATP-dependent protease FtsH, Mol. Cell 22 (2006) 575–585.
[41] K. Tunyasuvunakool, J. Adler, Z. Wu, T. Green, M. Zielinski, A. Zidek, A. Bridgland, A. Cowie, C. Meyer, A. Laydon, S. Velankar, G.J. Kleywegt, A. Bateman, R. Evans, A. Pritzel, M. Figurnov, O. Ronneberger, R. Bates, S.A.A. Kohl, A. Potapenko, A. J. Ballard, B. Romera-Paredes, S. Nikolov, R. Jain, E. Clancy, D. Reiman, S. Petersen, A.W. Senior, K. Kavukcuoglu, E. Birney, P. Kohli, J. Jumper, D. Hassabis, Highly accurate protein structure prediction for the human proteome, Nature 596 (2021) 590–596.
[42] M. Vostrukhina, A. Popov, E. Brunstein, M.A. Lanz, R. Baumgartner, C. Bieniossek, M. Schacherl, U. Baumann, The structure of Aquifex aeolicus FtsH in the ADP-bound state reveals a C2-symmetric hexamer, Acta Crystallogr. D Biol. Crystallogr. 71 (2015) 1307–1318.
[43] K. Westphal, S. Langklotz, N. Thomanek, F. Narberhaus, A trapping approach reveals novel substrates and physiological functions of the essential protease FtsH in Escherichia coli, J. Biol. Chem. 287 (2012) 42962–42971.
[44] M.D. Winn, C.C. Ballard, K.D. Cowtan, E.J. Dodson, P. Emsley, P.R. Evans, R. M. Keegan, E.B. Krissinel, A.G. Leslie, A. McCoy, S.J. McNicholas, G.N. Murshudov, N.S. Pannu, E.A. Potterton, H.R. Powell, R.J. Read, A. Vagin, K.S. Wilson, Overview of the CCP4 suite and current developments, Acta Crystallogr. D Biol. Crystallogr. 67 (2011) 235–242.